We are IntechOpen, the world's leading publisher of Open Access books Built by scientists, for scientists

4,800
Open access books available

122,000
International authors and editors

135M
Downloads

Our authors are among the

154
Countries delivered to

TOP 1%
most cited scientists

12.2%
Contributors from top 500 universities

CLARIVATE ANALYTICS BOOK CITATION INDEX INDEXED

WEB OF SCIENCE™

Selection of our books indexed in the Book Citation Index in Web of Science™ Core Collection (BKCI)

Interested in publishing with us?
Contact book.department@intechopen.com

Numbers displayed above are based on latest data collected.
For more information visit www.intechopen.com

18

Fuzzy Control of WT with DFIG for Integration into Micro-grids

Christina N. Papadimitriou and Nicholas A. Vovos
University of Patras/Electrical and Computer Engineering dpt.
Greece

1. Introduction

Few years ago Power Systems consisted mainly of large generation plants supplying distant loads through the utility grids. The last years, though, a number of factors lead this structure to change gradually. Small generators of some MW have been already dispersed (DGs) throughout the transmission grid. The distribution of smaller generation units throughout the distribution system as near as possible to the consumer loads has already begun. The DG, up to now, does not provide auxiliary services such as back-up power, voltage support and reliability of supply and its operation is kept under constant power factor equal to 1 at all times. During network disturbances, the DGs up to the present are disconnected until normal operation is reestablished. When the distributed generation penetration is high this may lead to system instability.

Therefore, the DG has to change from passive appendage of primary energy supplier to active sources remaining connected to the grid and offering ancillary services. In some countries legislation changed, so that DG remains connected during disturbances and supports the grid. Under this operating philosophy, DGs must support the grid during local disturbances, as central generation stations support high voltage systems in the transient period. This can be achieved through the control of the DGs electronic interface to the main grid and the energy storage plants. These controllable (centrally or distributed) DGs (<100kWe) connected to the distribution grid, together with the local energy storage devices and the local controlled loads comprise an active distribution grid, the so-called micro-grid. In other words, the micro-grid can be seen as a miniature of a large interconnected grid that can provide the demanded power and can also change from interconnected to islanded mode of operation (Soultanis, 2008) and vice-versa. The micro-grid concept is the effective solution for the control of grids with high level of DG penetration (Brabandere et al., 2007).

The control of the micro-grid has to be reliable, flexible and according to system specifications. The DGs of the micro-grid have to cooperate in order to cover the local load needs for active and reactive power either under local disturbances or under islanding operation mode. So, in order to achieve the full benefits from the operation of the controllable distributed generation, an hierarchical control system architecture comprising three control levels can be envisaged in a future micro-grid. The Micro source Controller (MC) is the controller of the first layer (peer-to-peer (Meiqin et al., 2008)) and uses local information to control the voltage and the frequency of the micro-grid in transient conditions. This way, any DG can be integrated into the micro-grid operating in «plug and

play» mode (Nikkhajoei& Lasseter, 2009). The Micro-grid Central Controller (MGCC) optimizes the micro-grid operation and the Distribution Management Systems (DMS) optimizes multiple MGCC which are interfaced in. As the proposed controller in this chapter is based on local information it comprises the MC of the micro-grid.
The usual peer-to-peer controller of the DGs converters uses the power vs. frequency droop characteristics in order to produce the active and reactive power reference combined with classical PI controllers, as it is mentioned in the review of state-of –the- art controllers in (Meiqin et al., 2008). In (Shahabi et al., 2009), the classical active power regulation takes into account the phase-locked loop (PLL) dynamics in order to prevent major oscillations from happening when a transition between grid connected mode and autonomous operation mode takes place. In (Brabandere et al., 2007) the primary, secondary and tertiary control algorithms are designed and tested in an experimental setup. The local controller uses the classical droop equation while the secondary and tertiary controllers aim at power quality and economic optimization respectively. The converters of the DGs communicate via the Internet. In (Nikkhajoei& Lasseter, 2009) the classical control is applied giving emphasis to the storage device algorithm, so that all micro sources have unified dynamic performance. In (Nishikawa et al., 2008) the classical local controller applied to the converters of a DFIG is combined with a pitch controller for a better dynamic response of a micro-grid at the mean voltage side. In (Katirarei & Iravani, 2006), the active power regulation is achieved through the classical controller combined with a frequency restoration strategy while three different strategies for reactive power regulation are adopted. The micro-grid dynamic behavior and the parameters of the DGs are mathematically investigated.
The droop equation combined with classical control can lead, under certain operational conditions, the micro-grid to instability while the stability enhancement for these cases needs sophisticated calculations (Mohamed& El- Saadany, 2008). In addition, the non-linearity of the micro-grid makes the implementation of fuzzy logic controllers at the DGs converters an attractive proposal. Moreover, fuzzy logic facilitates the «plug and play» operation for the DGs as the needed adjustments are minor due to the flexibility of fuzzy logic and easier due to the linguistic variables used.
This chapter presents a fuzzy based local controller so that a WT with DFIG is integrated into a micro-grid which is connected to a weak distribution grid. The micro-grid under study is simulated with Matlab/Simulink software, considering a micro-grid as it is described in (Meiqin et al., 2008). The micro-grid includes a hybrid fuel cell-battery system and a WT with DFIG. Firstly the micro-grid response is recorded, when a local disturbance (step load change) happens and secondly, when a transition from interconnected mode to islanding operating mode occurs. In a few seconds the grid is reconnected and the controllers' performance is evaluated again.
In the following section the micro-grid architecture is presented. In the fourth section the WT with the DFIG system is presented and some key points about its operation are discussed. In the fifth section, the designed controller based on fuzzy logic is analyzed. In the sixth section the simulation results are presented and the last section concludes the chapter.

2. Micro-grid structure

The micro-grid concept was put forward in 2001. Since then several micro-grids with multi-energy generators (MGMEG) and storages have been built in labs in universities and

institutes all over the world (Meiqin et al., 2008). The majority of the DGs are connected to the micro-grid via electronic converters e.g. voltage source inverters (VSI). Internal combustion engines, gas turbines, micro turbines, photovoltaic, fuel cells and wind turbines constitute different technology micro sources. Micro sources have different dynamics depending on the prime mover size and the technology used. In this chapter the structure of the simulated micro-grid resembles those developed in the labs and includes two different micro sources (Fuel Cell System (FCS)-Battery and WT with DFIG). The reasons that led to the selection of these micro sources and especially of the WT with the DFIG will be explained later in details. As seen in (Bathaee & Abdollahi, 2007), the micro-grid architecture that combines different DGs is more practical as the storage device equipment or controllable loads can be reduced. The FCS (with proton exchange membranes (PEM)), that is combined with a battery bank forming a hybrid system, is connected to the AC feeder via a VSI and the WT with DFIG is connected directly to the feeder. In both DGs the "peer-to-peer" controller is based on fuzzy logic and the VSI local controllers are designed in "plug and play" operation mode. The designed controllers for the hybrid system are presented in a former paper of the authors and the controllers of the WT with DFIG are presented in section 5 of this chapter. The "peer-to-peer" controllers imply that through the electronic interface the DGs can provide the local grid with the demanded active and reactive power in absence of a central controller and communication links among micro sources. The "plug and play" operation mode implies that a micro source can be added to the micro-grid without reengineering the control and protection of units that are already part of the system. It is expected that in steady state a micro-grid central controller should coordinate DG to optimize operation, minimizing active power losses and maintaining flat voltage profile. The structure of the micro-grid under study is presented in Fig. 1. The micro-grid data are given in the following.

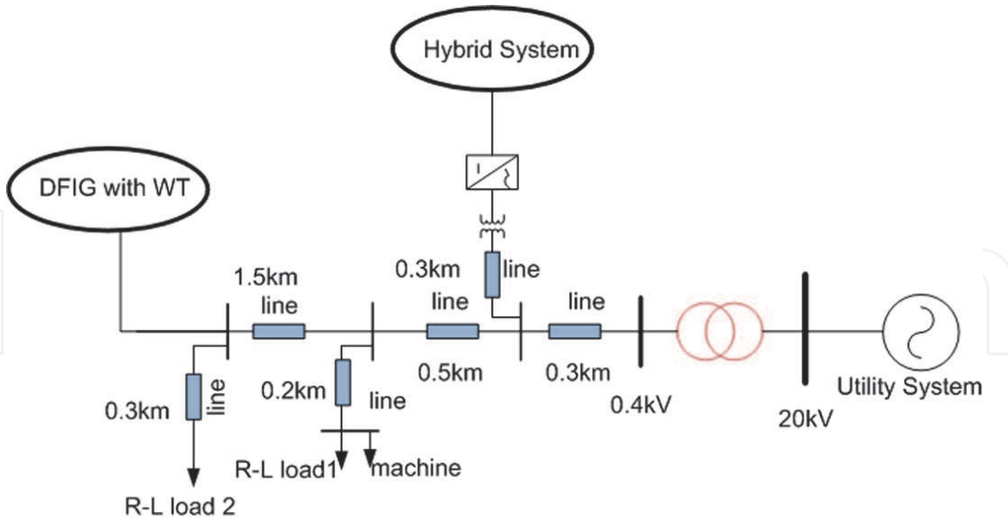

Fig. 1. Micro-grid Structure.

FCS PEM: 30 kW, 200 cells, 200A, 150V, 280cm^2/cell.
DC Motor for the air supply system: 5 hp, 500 V, 1750 rpm, field: 300 V
Battery Bank: 234 HV Nickel-Metal Hybrid cells of 1.2 V, 2 Ah, 280 V.
Transformer: 50kVA, 190:380 V, 50 Hz.

WT with DFIG: The parameters of the electric models were adopted from SimPowerSystems library of Matlab/Simulink.
Doubly Fed Induction Generator: 75 kW, 400 V, 50 Hz, 1484 rpm, H=0.2, F=0.012, p=2.
WT: nominal mechanical output power: 80 kW, base wind speed: 12 m/sec, nominal rotor speed: 18rpm.
Distribution lines*:* AAAC type (4*185), X=0.236 Ω/km, R=0.204 Ω/km
AC system*:* 380 V, 50 Hz, base p.u.:100 kW, 380 V.
R-L load1: 37kW, 13kVar, 380 V
R-L load2: 36kW, 10kVar, 380 V
Squirrel- Cage Induction Motor: 20hp, 400 V, 50 Hz, 1460 rpm

3. Wind turbine with doubly fed induction generator

3.1 Advantages of the DFIG structure

The DFIG system presents the following attractive advantages:

- The active and reactive power can be controlled independently via the current of the rotor.
- The magnetization of the generator can be achieved via the rotor circuit and not necessarily via the grid.
- The DFIG is capable of producing reactive power that it is delivered through the grid-side converter. Usually, this converter operates under constant unity power factor and it is not involved in reactive power trading with the grid. Also, the DFIG can be regulated in order to produce or consume a certain amount of reactive power. This way, the voltage control is achieved in cases of weak distribution grids.
- The converter size is not determined according to the total power of the generator but according to the decided speed range of the machine and therefore the slip range. For example, if the speed range is controlled between ±30% of the nominal speed, the nominal power of the converter is equal to the 30% of the nominal power of the generator. The selected speed range is decided according to the economical optimization and the increased performance of the system.

In the present study, the WT with the DFIG has been selected for integration into the micro-grid whose structure has already been presented. Beyond the technical advantages that the DFIG system presents, the practical reasons that led to this selection are the following:

- The micro-grid can operate under islanding mode either because of a fault at the mean voltage side or because of grid maintenance. Therefore, the microsources have to support the local grid in active and reactive power without stalling. But the microsources based on different technologies, have varying time constants. So, slow response microsources co-exist with fast response microsources in the same micro-grid structure for reliability purposes. In this study, the hybrid FCS has large time constant. The existence of the WT with the DFIG in the same micro-grid prevents the hybrid system from stalling during disturbances as the kinetic energy stored in the moving parts of the WT is exploited.
- As already mentioned, the control of DFIG is remarkably flexible through the electronic devices supporting the frequency and the voltage of the local grid. A well designed control can lead to greater power delivery (exploiting the machine inertia) than in any other type of WT.

- The DFIG technology decouples the electrical from the mechanical parts. So, in cases of frequency fluctuations of the grid, the operation of the WT with the DFIG is not affected except from the case that the control imposes a different operation. This way, the WT with DFIG can change smoothly through different operating modes when this is asked by the control system. The last is useful in the micro-grid concept.

3.2 WT with DFIG configuration

The Doubly Fed Induction Generator system can independently provide voltage and frequency regulation capabilities via the rotor current control as already mentioned. The basic configuration of the WT with DFIG is presented in Fig. 2.
The AC/DC/AC converter is divided into two components: the rotor-side converter (C_{rotor}) and the grid-side converter (C_{grid}). C_{rotor} and C_{grid} are Voltage-Sourced Converters that use forced-commutated power electronic devices (IGBTs) to synthesize an AC voltage from a DC voltage source. A capacitor connected on the DC side acts as the DC voltage source. A coupling inductor L is used to connect C_{grid} to the grid. The three-phase rotor winding is connected to C_{rotor} by slip rings and brushes and the three-phase stator winding is directly connected to the grid. The power captured by the wind turbine is converted into electrical power by the induction generator and it is transmitted to the grid by the stator and the rotor windings. The mathematical equations of the wind turbine model are given below.

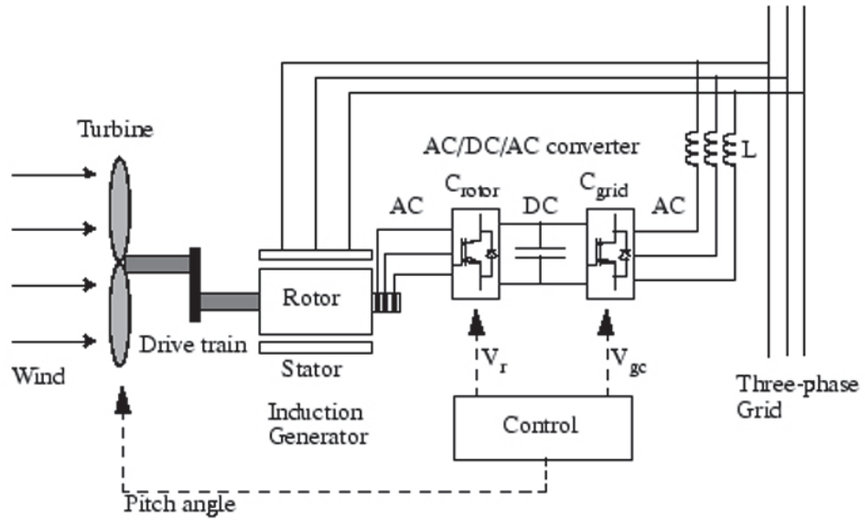

Fig. 2. The WT with the DFIG structure.

The power obtained from a given wind speed is expressed by the following equation:

$$P_w=0.5\rho\pi R^2v^3C_p(\lambda,\beta) \quad (1)$$

with ρ being the air density, R the effective area covered by the turbine blades, v the mean value of the wind speed at the height of the rotor axis, C_p the power coefficient of the wind turbine and β the pitch angle.
The tip speed ratio is defined as:

$$\lambda=\omega_w R/v \quad (2)$$

The mechanical torque is defined as:

$$T_w=P_w/\omega_w \quad (3)$$

with ω_w being the wind turbine rotor speed.
The coefficient C_P is defined as:

$$C_p=c_1(c_2/\lambda-c_3\beta-c_4)e^{-c5/\lambda}+c_6\lambda \quad (4)$$

where the coefficient values are:
c1 = 0.5176, c2 = 116, c3 = 0.4, c4 = 5, c5 = 21 και c6 = 0.0068.
The model of the converters is the analytical model for voltage source converters given in the software package Matlab/Simulink (SimPowerSystems library). The wound induction generator model and its parameters were adopted by the same library, too.

3.3 Exploiting the kinetic energy

Among the different wind energy conversion systems, WTs with DFIG can provide the required services without the need of large costs of the power electronics hardware, if adequate control strategies are added (Shahabi et al., 2009). The control flexibility due to the DFIG electronic converter makes it possible to define various control strategies for participation in primary frequency control and voltage regulating support. A well designed control can deliver greater power exploiting the machine inertia than the delivered power from any other type of WT. So, the kinetic energy stored in the moving parts of the WT can be delivered if needed via the adequate controller.
The classical control of the wind power systems aims at the maximum power absorption for the whole wind speed range. However, if the wind turbines are part of the micro-grid, they have to provide frequency and voltage support to the local grid. There are several techniques for controlling the delivered power by the WT. In some papers, (Morren et al., 2006), during transients, the exploitation of the kinetic energy is achieved for a short time period and the optimum operation of the WT is shortly restored. In (Bousseau et al., 2006), pitch control is used so that the power delivering range increases in high wind speeds and the rotor speed increases in low wind speeds. In this study, pitch control is not applicable, as the wind speed is below the predefined limit (12m/s) and the angular position of the pitches doesn't change. Moreover, the time constant of the last action would be larger than the desirable time constant for the present study.
So, in order for a permanent control to be integrated in the WT with the DFIG, a slight de-optimization of the power production of the WT has been selected (Janssens et al., 2007).This way, a margin for excess power delivery during transients through the kinetic energy exploitation is created. In Fig.3, the means for de-optimizing the WT operation are presented graphically. The graph presents the mechanical power as a function of the rotor speed for given wind speeds and for pitch control equal to zero.
The A point corresponds to the WT operation at the optimum rotor speed. The de-optimization of the rotor speed is achieved either by imposing operation at a lower speed (point B-deceleration) or by imposing operation at a higher speed (point C-acceleration). In this study, the acceleration has been chosen as the deceleration of the rotor presents the following drawback: the delivered active power is originally degraded (the point of operation moves towards the opposite direction) while the rotor is trying to accelerate. This phenomenon is presented in Fig.4.

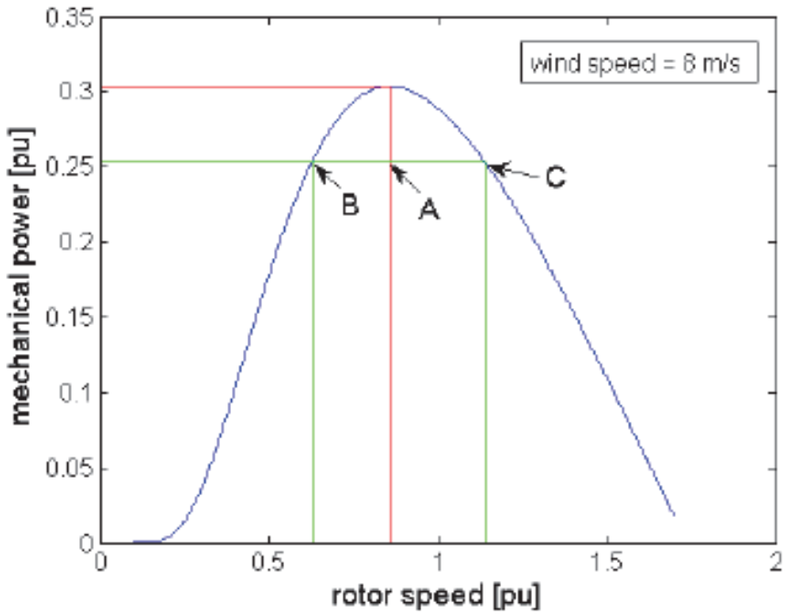

Fig. 3. Means of increase of the power margin (Janssens et al., 2008).

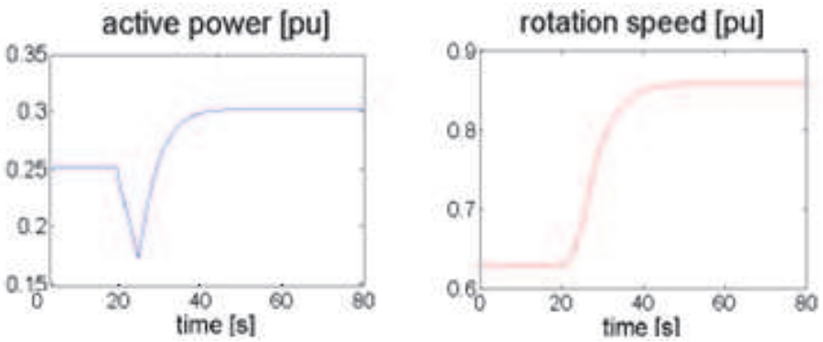

Fig. 4. Active power and rotation speed during the deceleration technique (Janssens et al., 2007).

On the contrary, during the acceleration technique, the desirable active power is delivered immediately. This advantage is of great significance as it prevents the stalling of micro sources with large time constants such as FCS during transients. This phenomenon is presented in Fig.5. The active power overshooting is noticed due to the absorption of the kinetic energy during acceleration.

4. Control design based on fuzzy logic

4.1 Why fuzzy logic?

As it is briefly mentioned in the introduction, the local controllers are based on fuzzy logic due to its flexibility and adaptiveness and due to the non-linearity of the system. The fuzzy controllers are non linear in nature and it is expected to have a robust performance under disturbances. Analytically, the four main flow subsystems of the FCS and the auxiliary

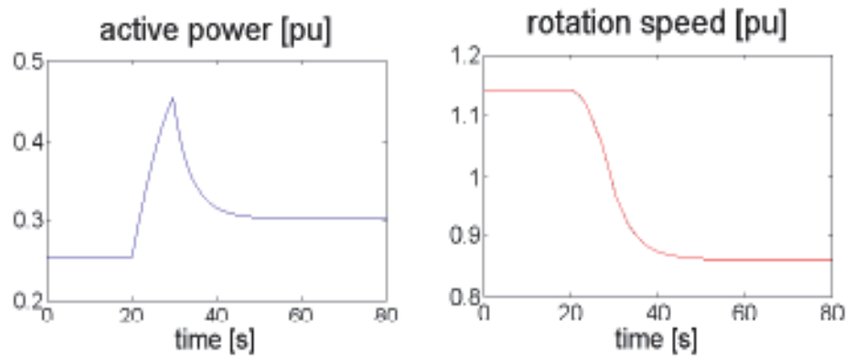

Fig. 5. Active power and rotation speed during the acceleration technique (Janssens et al., 2007).

subsystems establish a non linear FCS. In addition, the presence of non linear and cross-coupling terms of the DFIG dynamics form a micro-grid intensively non linear. Some key points of great significance for the system efficiency and performance outlined below enhance the application of a fuzzy based intelligent control. As for the hybrid FCS, it is significant for the compressor motor controller to have a good dynamic response during fast load changes so that the FCS voltage does not drop dramatically leading to oxygen starvation. Secondly, the controller for the system self-powering has to act simultaneously with the fuel flow control achieving stability and accuracy while minimizing overshooting and current rippling. The VSI controllers of the WT with DFIG and of the hybrid FCS have to meet the same requirements too. The design of the fuzzy controllers does not require a precise mathematical modeling or sophisticated computations that in many cases lack of efficiency and good performance. The last remark makes fuzzy logic suitable and practical in real systems where the engineer tunes the local controller easier via the linguistic variables (easy engineering).

The fuzzy controllers are designed from a heuristic knowledge of the system. Of course, they are thoroughly iterated by a system simulation study in order to be fine tuned. The advantage of this method is the fast convergence as it provides adaptively decreasing step size in the search of the adequate output. Besides, noisy and varying input signals do not affect the search. So, the weights of the membership functions (MFs) of every controller were chosen after qualitative knowledge of the simulation system. Triangular MFs were chosen as the most popular type providing satisfactory results. It can be seen in the following section that the MFs are asymmetrical, giving more sensitivity as the variables approach zero values. The defuzzification method that is followed is the Centre of Area (COA) defuzzifier.

4.2 Fuzzy local controllers

The current control of a machine is achieved mainly by means of vector control in a dq frame. The same technique is adopted in this chapter. The desired dimensions are firstly converted into vector components and secondly they are converted in AC components in order to be used in the PWM technique. In order to control the rotor current of a WT with DFIG by means of vector control, the reference frame has to be aligned with a flux linkage. One common way is to control the rotor currents with stator-flux orientation. If the stator resistance is considered to be small, stator-flux orientation is aligned with stator voltage. The

applied vector control is based on a synchronously rotating, stator-flux oriented d-q reference frame, which means that the d-axis is aligned with the vector of the stator magnetic flux of the stator and the q component is zero.
The DFIG controller of this study consists of the control applied to the grid-side converter (C_{grid}) and the control applied to the rotor-side converter (C_{rotor}).

4.2.1 C_{rotor} control

This control regulates independently the active and reactive power of the stator according to the following equations:

$$P_s = \frac{3}{2}\left(u_{ds}i_{ds} + u_{qs}i_{qs}\right) = \frac{3}{2}u_{qs}i_{qs} = -\frac{3}{2}u_{qs}\frac{L_m}{L_s}i_{qr}$$
$$Q_s = \frac{3}{2}\left(u_{qs}i_{ds} - u_{ds}i_{qs}\right) = \frac{3}{2}u_{qs}i_{ds} = \frac{3}{2}u_{qs}\frac{\lambda_{ds} - L_m i_{dr}}{L_s} \quad (5)$$

As it can be seen, the active power is regulated via the q component of the rotor current and the reactive power via the corresponding d component. The control configuration is shown in Fig.6. Three fuzzy controllers (Fc) were designed in order to accomplish the desired control. Due to the flexibility of the fuzzy logic the same fuzzy controller (Fc5a) with the same membership functions (MFs), controls both d and q component of the rotor voltage. The MFs weights are different though.

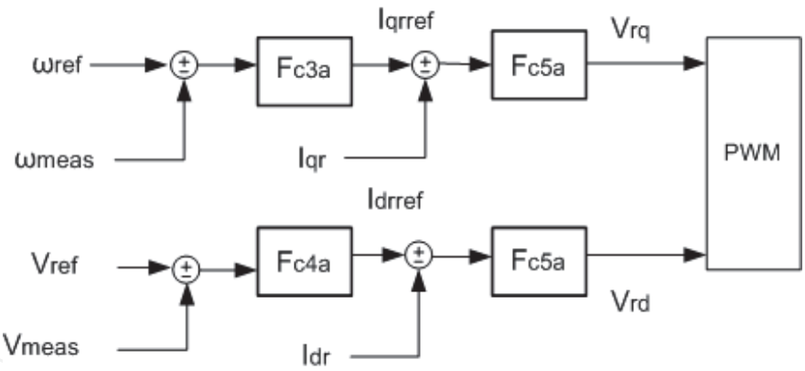

Fig. 6. General configuration of the control for the Rotor side Converter.

The classical maximum power point tracking control of the WT determines the reference value of the power so that the generator speed has its optimum value for certain wind speed. In this study, the deviation of the frequency measured at the DFIG output has been incorporated into the active power controller and the generator speed is different from its optimum value. Therefore the WT with DFIG can instantly supply more power to the local grid in case of emergency by losing speed.
Fc3a: As seen in Fig. 6 the input of this controller is the deviation of the angular velocity measured at the DFIG output from its reference. The output of the Fc3a is the deviation of the q component (ΔI_{qrref}) of the reference value of the rotor current, I_{qrref}. The ΔI_{qrref} signals are added together in every simulation step in order to comprise the I_{qrref} value (in p.u.) according to the following equation:

$$I_{qrref}^{new} = I_{qrref}^{old} + \Delta I_{qrref} \quad (6)$$

where I_{qrref}^{new} being the new value of the control signal and I_{qrref}^{old} being the old value of the control signal.

The fuzzy input variables of the Fc3a are expressed by the following linguistic variables: : "very positive (VP)", "medium positive (MP)", "positive (P)", "ok (OK)", "negative (NEG)", "medium negative (MNEG)", "very negative (VNEG)". The fuzzy variables of the output of the Fc3a are expressed by the following linguistic variables: "high positive (POS_H)", "medium positive (POS_M)", "low positive (POS_L)", "ok (OK)" ,"high negative (NEG_H)", "medium negative (NEG_M)", "low negative (NEG_L)". The membership functions of the input and the output are shown in Figs. 7 and 8 respectively.

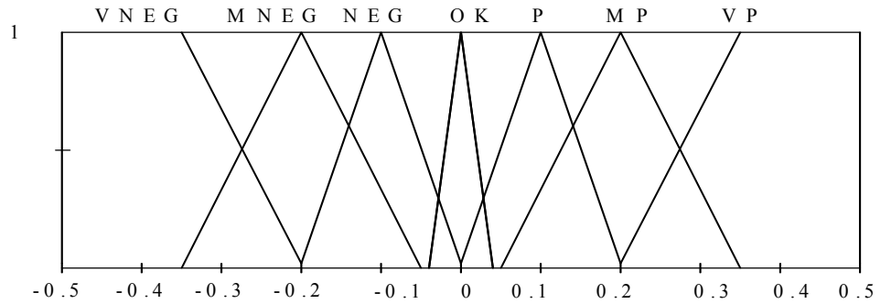

Fig. 7. Membership functions of the input signal of Fc3a.

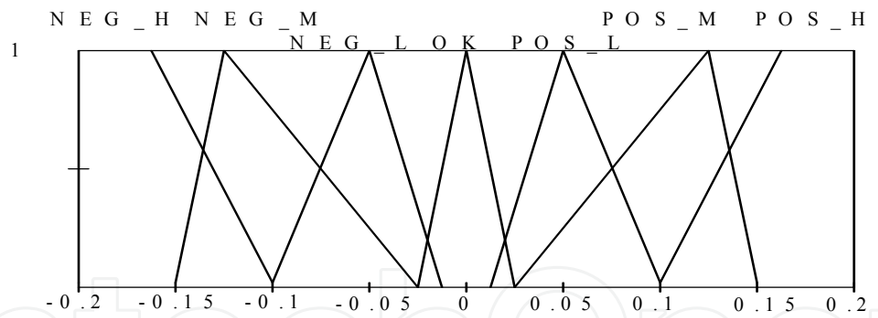

Fig. 8. Membership functions of the output signal of Fc3a.

The 7 fuzzy rules are presented in the following table:

Fc3a Input	VP	MP	P	OK	NEG	MNEG	VNEG
Fc3a Output	POS_H	POS_M	POS_L	OK	NEG_L	NEG_M	NEG_H

Table 1. Fuzzy Rules of Fc3a.

Fc5a: As seen in Fig. 6 the input of this controller is the difference between the reference and the measured q (or d) component of the rotor current ((I_{qrref}- I_{qr}) or (I_{drref}- I_{dr})). The output of the Fc5a is the deviations of the q (or d) component of the rotor voltage control (ΔV_{rq} or

ΔV_{rd}). The ΔV_{rq} or ΔV_{rd} signals are added together in every simulation step in order to comprise the V_{rq} or V_{rd} value (in p.u.) according to an equation similar to equation (6).
The fuzzy variables of the Fc5a are expressed by the same linguistic variables as Fc3a.The membership functions of the input and the output are shown in Figs. 9 and 10 respectively. The 7 fuzzy rules of the Fc5a are the same as those of the Fc3a.

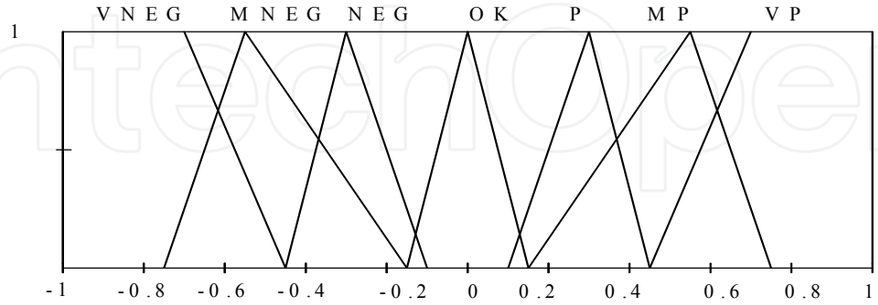

Fig. 9. Membership functions of the input signal of Fc5a.

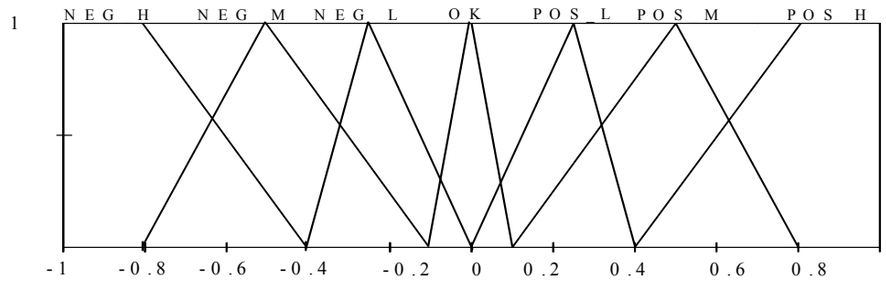

Fig. 10. Membership functions of the output signal of Fc5a.

Fc4a: The input of this controller is the difference between the measured voltage at the generator output and the reference value (V_{ref}- V_{meas}). The output of this controller is the variations of the d component of the reference value of the rotor current ΔI_{drref}. The reference value of the rotor current I_{drref}, is formed as already mentioned
The fuzzy variables of the Fc4a are already described. The membership functions of the input and the output are shown in Figs. 11 and 12 respectively. The 7 fuzzy rules of the Fc4a are the same as those of Fc3a.

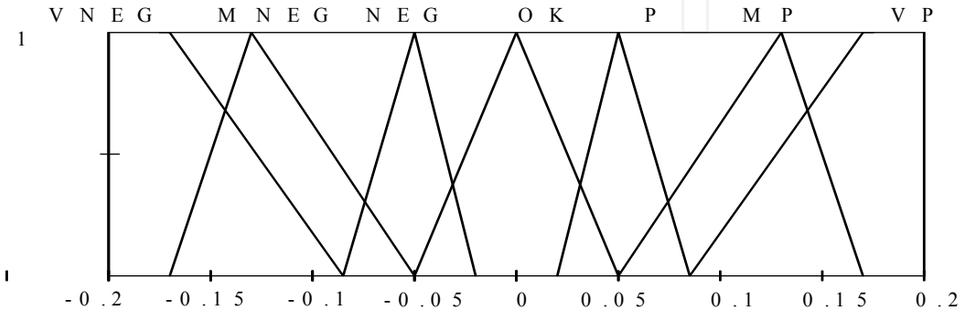

Fig. 11. Membership functions of the input signal of Fc4a.

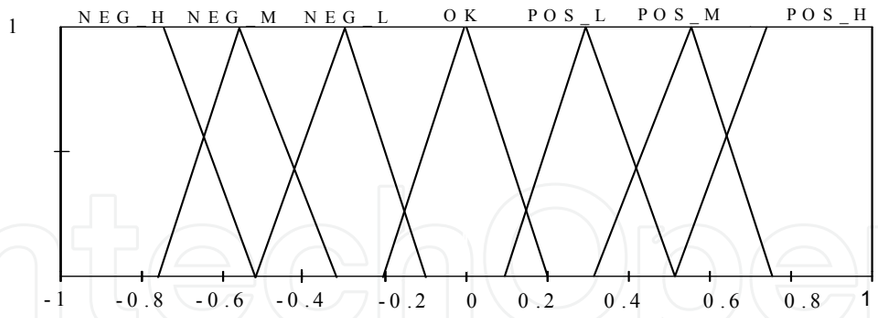

Fig. 12. Membership functions of the output signal of Fc4a.

4.2.2 C_{grid} control

As the stator resistance is considered to be small, stator-flux orientation is the same with the stator voltage orientation. The applied vector control, in this case, is based on a synchronously rotating, stator-flux oriented d-q reference frame, which means that the d-axis is aligned with the vector of the grid voltage and the q component is zero. This control also regulates independently the active and reactive power according to the following equations:

$$\begin{aligned} P_s &= \frac{3}{2}\left(u_{gd}i_{gd} + u_{gq}i_{gq}\right) = \frac{3}{2}u_{gd}i_{gd} \\ Q_s &= \frac{3}{2}\left(u_{gq}i_{gd} - u_{gd}i_{gq}\right) = -\frac{3}{2}u_{gd}i_{gq} \end{aligned} \tag{7}$$

The control configuration is shown in Fig.13. Two fuzzy controllers (Fc) were designed in order to accomplish the desired control. Due to the flexibility of the fuzzy logic the same fuzzy controller (Fc2a) with the same membership functions (MFs), controls both d and q component of the grid voltage. The MFs weights are different though. This control regulates the independent exchange of active and reactive power between the converter and the local grid. The local controllers focus on regulating the dc link voltage and the ac grid voltage. The d component of the converter current regulates the dc-link voltage and the q component of the converter current regulates the reactive power.

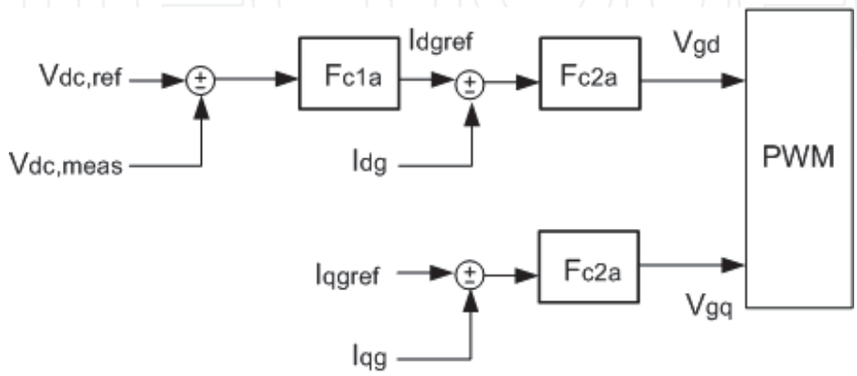

Fig. 13. General Configuration of the control for the Grid side Converter.

Fc1a: As seen in Fig.13 the input of this controller is the difference between the measured dc link voltage and the reference value ($V_{dc,ref}$-V_{dc}). The output of this controller is the deviation of the reference value of the d component of the output current (from the grid side) ΔI_{dgref}. The signal I_{dgref} is formed as already described.
The membership functions of the input and the output are shown in Figs. 14 and 15 respectively.

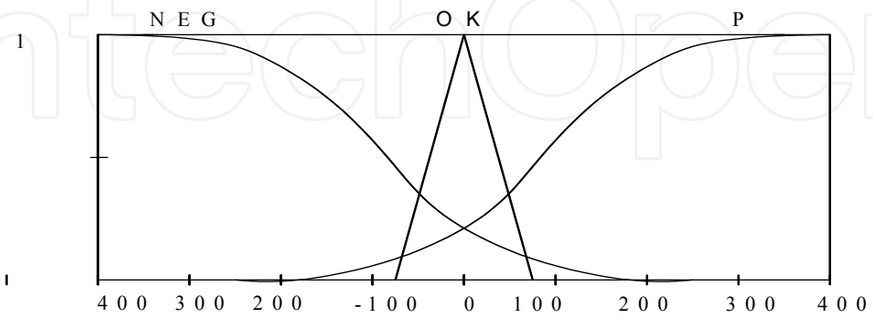

Fig. 14. Membership functions of the input signal of Fc1a.

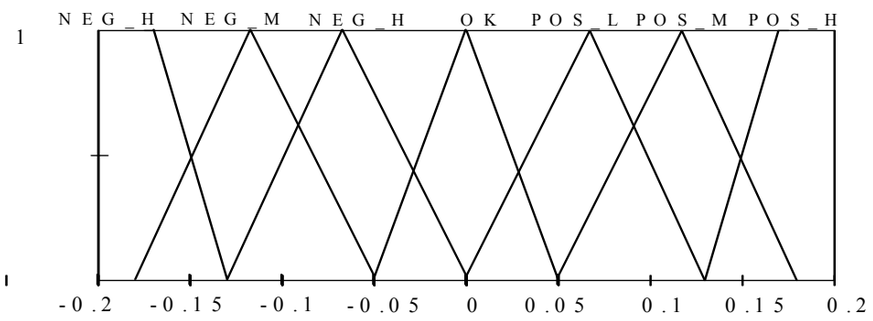

Fig. 15. Membership functions of the output signal of Fc1a.

The 7 fuzzy rules are presented in the following table:

Fc1a Input	P	P	P	OK	NEG	NEG	NEG
Fc1α Output	POS_H	POS_M	POS_L	OK	NEG_L	NEG_M	NEG_H

Table 2. Fuzzy Rules of Fc1a.

Fc2a: The input of this controller is the difference between the measured value of the q (or d) component of the output current and the reference value ((I_{qgref}-I_{qg}) or (I_{dgref}-I_{dg})). The output is the deviation of the q (or d) component of the voltage from the grid side (ΔV_{gq} or ΔV_{gd}). The control signal V_{gd} (or V_{gq}) is formed from the deviations as mention previously.
The reference value of the q component of the output current I_{qgref} is zero as the reactive power regulation through the C_{rotor} is preferred so that the electronic components rating remain small. Moreover, limiters are placed so that the currents don't exceed the electronic components specifications.

The membership functions of the input and the output are shown in Figs. 16 and 17 respectively.

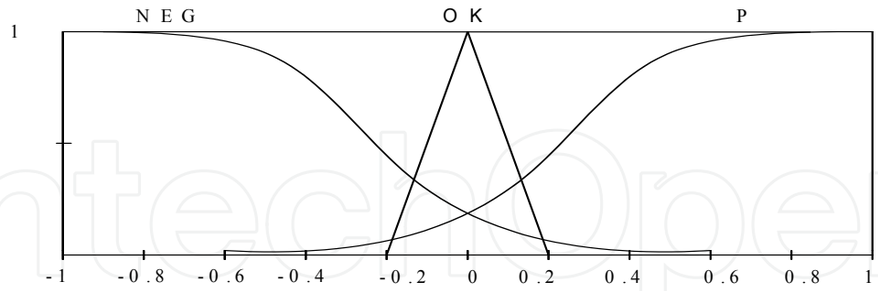

Fig. 16. Membership functions of the output signal of Fc2a.

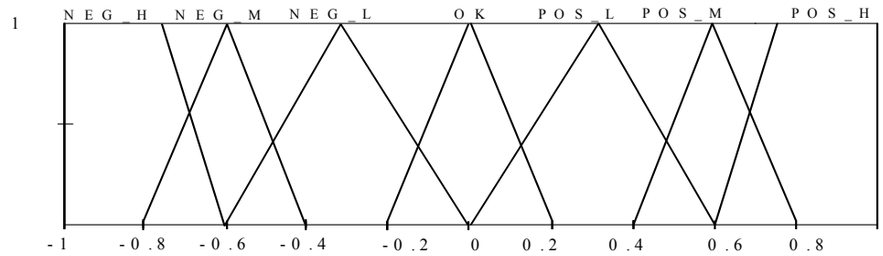

Fig. 17. Membership functions of the input signal of Fc2a.

The 7 fuzzy rules of the Fc2a are the same as those of Fc1a.

5. Simulation results

The data for the micro-grid are already given. In steady state the micro-grid is interconnected with the distribution grid and the initial steady state is the same for both cases studied. The R-L loads absorb their nominal active and reactive power and the induction motor operates at a slip of 2% and absorbs 10kW and 3kVar. 14% of the active power and almost a 100% of the reactive power of the loads are fed by the distribution grid. The DFIG feeds almost the 65% of the demanded active power and the hybrid system feeds the rest 21%. The DGs don't provide the loads reactive power during the interconnected mode of operation. The p.u. bases are: P_β=100 kW, V_β=380 V.

5.1 Local disturbances under grid-connected mode

At 0.5 sec, a step change of the mechanical load of the induction generator is imposed. The mechanical load is tripled and the DGs are offering ancillary services. The load sharing between the two DGs depends firstly on the dynamic response of each micro source and secondly on the weights of the MFs of the local controllers. In Fig.18, the measured frequency in steady state and during transient is presented. At 0.5 sec, the frequency drops due to the unbalance of active and reactive power in the system and returns to its nominal value after some oscillations within less than 0.5 sec. In Fig.19, the measured voltage at the point of common coupling (PCC) in steady state and during transient is presented. At the 0.5 sec, the voltage drops due to the unbalance of active and reactive power in the system and returns to its nominal value after some oscillations within 0.5 sec.

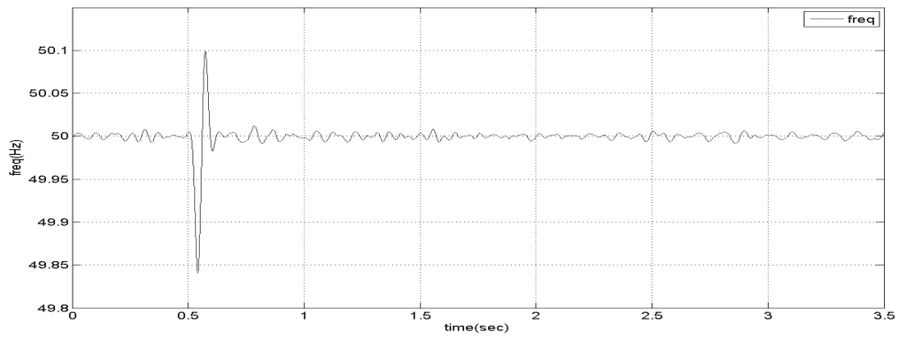

Fig. 18. The measured frequency.

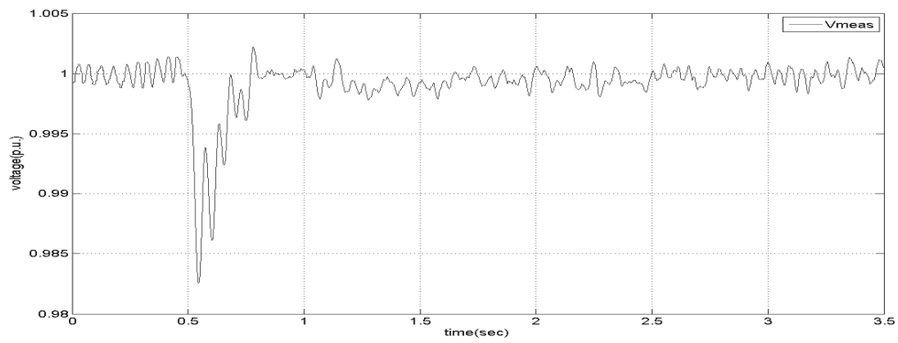

Fig. 19. The measured voltage at the PCC.

In Figs.20-22 the delivered active power by the grid, by the WT with the DFIG and by the hybrid FCS at the inverter's output are presented.

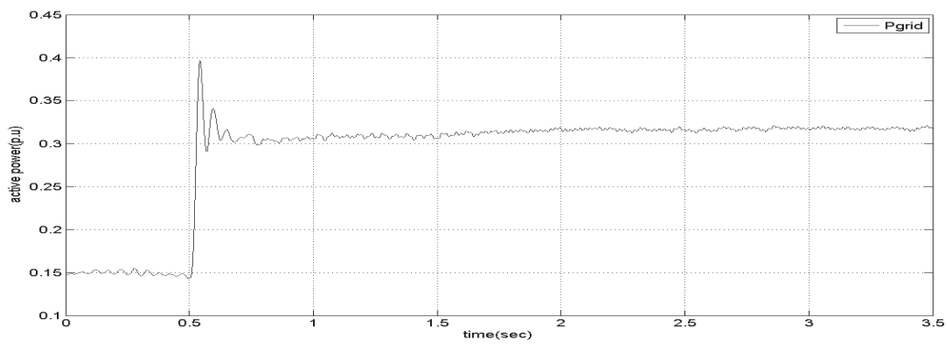

Fig. 20. The delivered active power by the weak distribution grid.

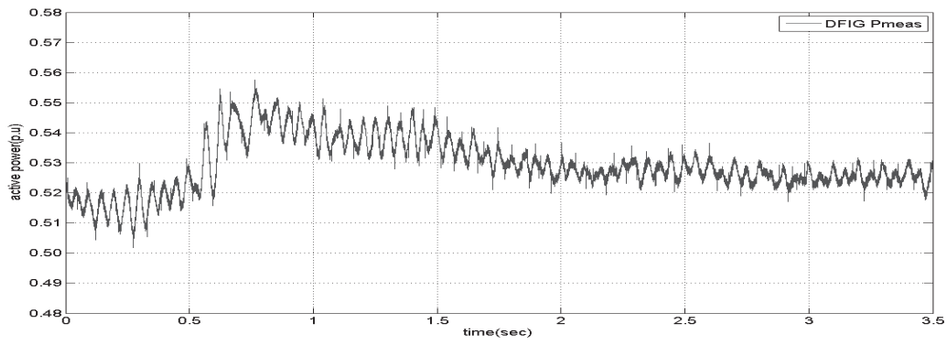

Fig. 21. The delivered active power by the WT with the DFIG.

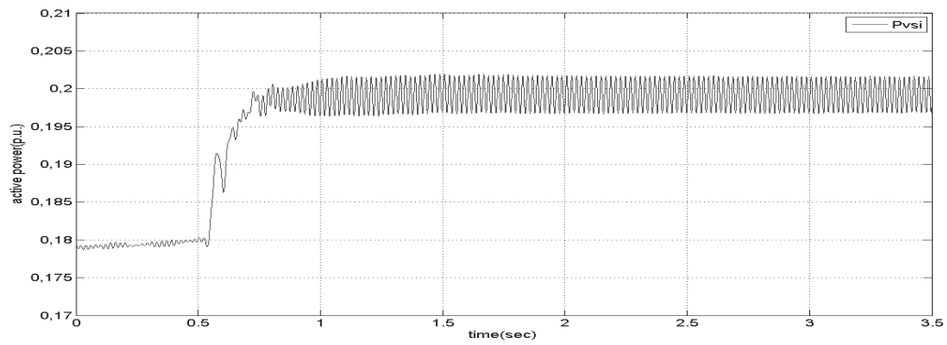

Fig. 22. The delivered active power by the hybrid FCS.

The grid (Fig.20) doubles the delivered active power and in the new steady state delivers about 30 kW. The WT with the DFIG (Fig.21) also increases the delivered power immediately to 55 kW because of the kinetic energy loss and after 1.5 sec from the disturbance it reaches a new steady state value (53 kW). Note the overshoot of the active power in the same figure. This happens due to the acceleration of the rotor technique already mentioned in a previous section. In Fig.22, the measured delivered power at the

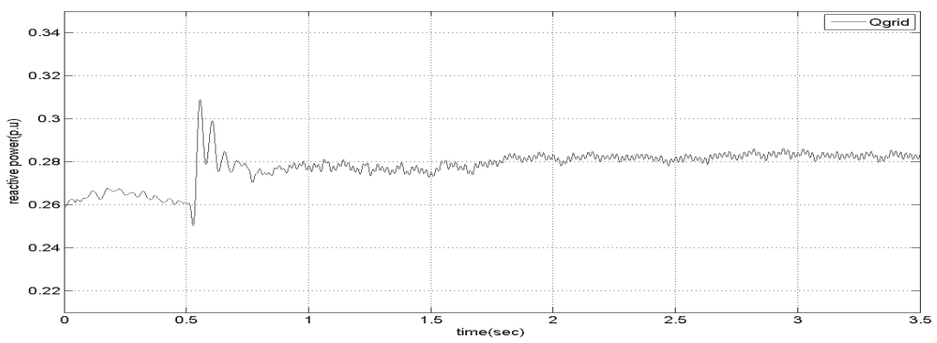

Fig. 23. The delivered reactive power by the weak distribution grid.

hybrid's FCS output is presented. Note that the fast response of the hybrid FCS is due to the existence of the battery at the dc-side. In the new steady-state the power demand has raised almost 26%. In total, the distribution grid covers the 29% of the active power demand, the WT covers the 51% and the hybrid FCS covers the remaining 20 %.
In Figs.23-25 the delivered reactive power by the grid, by the WT with the DFIG and by the hybrid FCS at the inverter's output are presented.

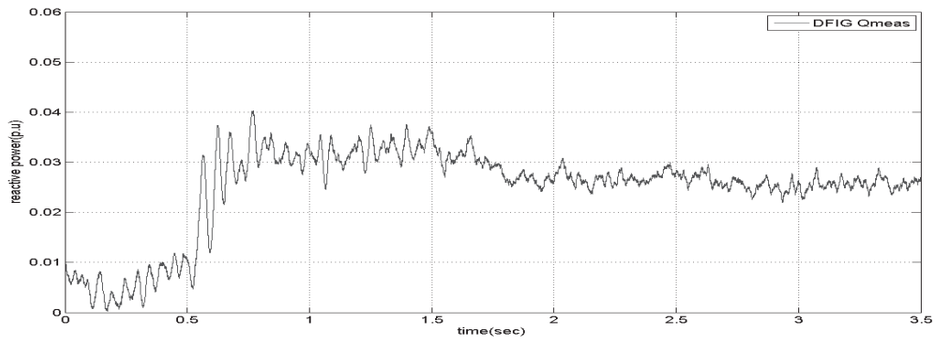

Fig. 24. The delivered reactive power by the WT with the DFIG.

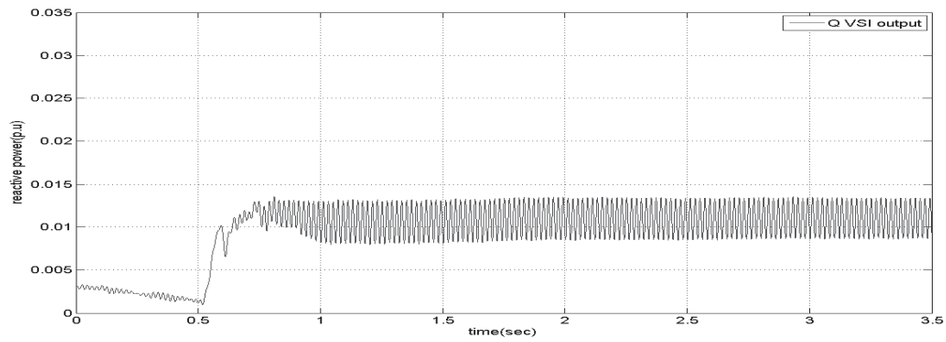

Fig. 25. The delivered reactive power by the hybrid system.

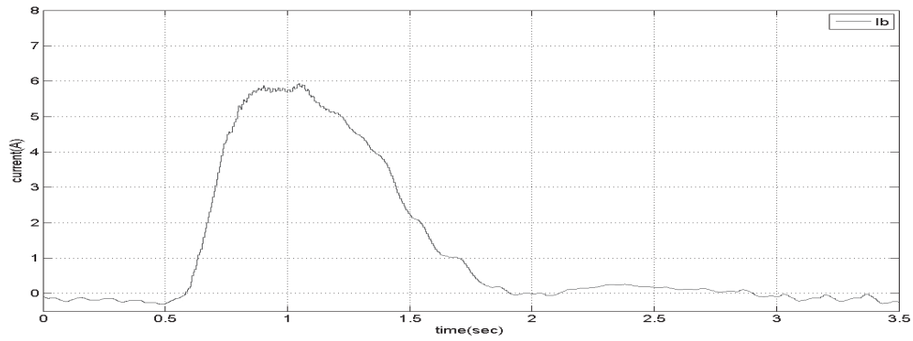

Fig. 26. The battery bank current in steady state and transient period.

In Fig.26 the battery bank current is presented. The battery bank current increases rapidly, in order to supply the battery the demanded power and returns to zero within 2 sec. In Fig.27, the FCS active power is presented. The FCS active power increases slowly in order to cover the total load demand and reaches a new steady state within 2 sec.

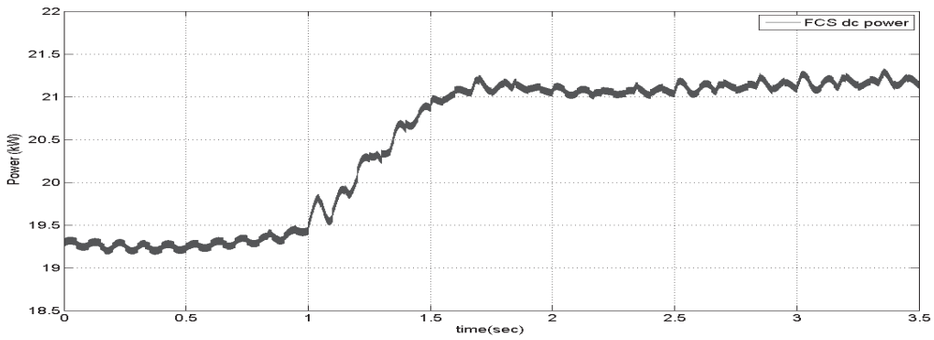

Fig. 27. The FCS active power delivered.

In Fig.28, the WT rotor speed is presented. Because of the disturbance imposed at the 0.5 sec, the rotor looses kinetic energy and reaches a new steady state.

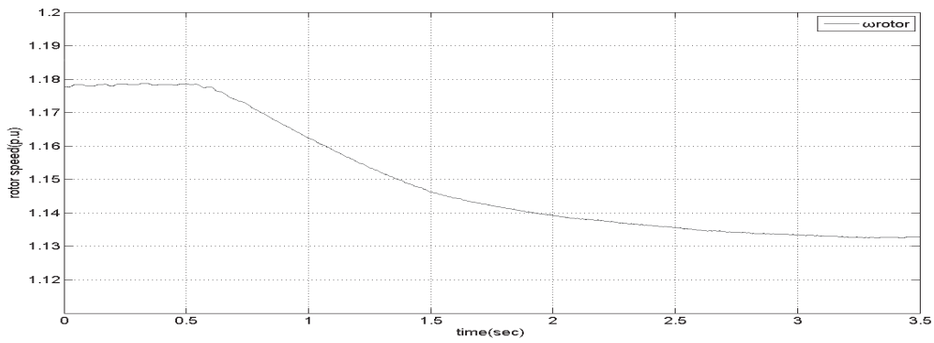

Fig. 28. The WT rotor speed in steady state and during transients.

In Fig.29, the control signals of the rotor side controller are presented in the same graph.

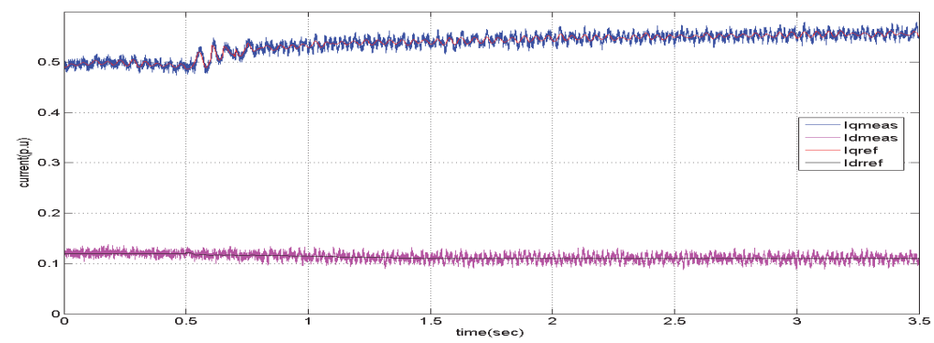

Fig. 29. The control signals of the rotor side controller.

5.2 Transition from grid-connected mode to islanding operating mode and transition from islanding operating mode to grid-connected mode

The initial steady state is the same as in the previous study case. At 0.5 sec, the grid is disconnected due to a fault at the mean voltage side or because of an intentional disconnection (e.g. maintenance work) and the micro sources cover the local demand. At 1.5 sec, while the system has reached a new steady state, the distribution grid is re-connected and finally a new steady state is reached. Note that, a micro-grid central control should lead the system to an optimal operation later.

In Fig.30, at 0.5 sec, the frequency drops due to the unbalance of active and reactive power in the system caused by the grid disconnection. The signal returns to its nominal value after some oscillations within 1sec. A small static error from the nominal value occurs but it is within the acceptable limits. At 1.5 sec. the distribution grid is re-connected with the micro-grid. An overshooting of this signal can be observed due to the magnitude and phase difference of the frequency of the two systems. Within 0.2 sec the micro-grid is synchronized with the distribution grid and the frequency reaches its nominal value of 50 Hz.

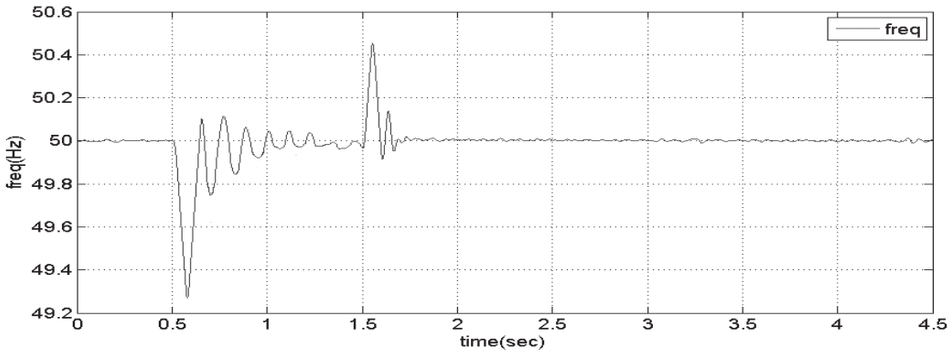

Fig. 30. The measured frequency.

In Fig.31 the voltage drops due to the unbalance of active and reactive powers in the system caused by the grid disconnection. The signal returns to its nominal value (a small static error is observed) after some oscillations within 1sec. At 1.5 sec. the distribution grid is re-connected with the micro-grid and the synchronization with the micro-grid is achieved after 3 sec.

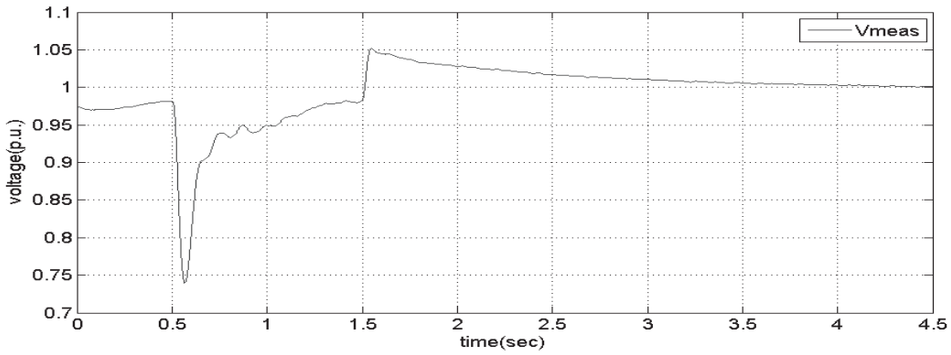

Fig. 31. The measured voltage at the PCC.

In Fig. 32-34 the delivered active power by the grid, by the WT with the DIFG and by the hybrid FCS at the inverter's output are presented. In Fig.32 the distribution grid is disconnected at 0.5 sec and is reconnected at 1.5 sec. In Fig.33 and 34, at 0.5 sec, the WT with the DFIG and the hybrid FCS increases the delivered power in order to eliminate the unbalance of power. At 1.5 sec, the grid is reconnected and the microsources are forced to regulate their delivered power so that the voltage and the frequency return to their nominal values.

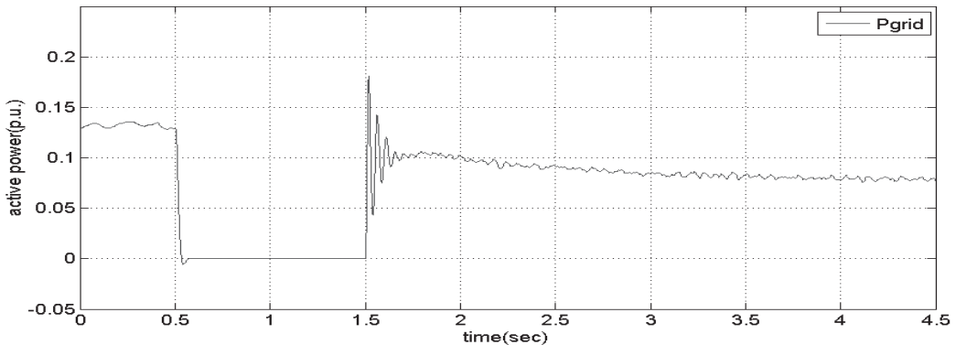

Fig. 32. The delivered active power by the weak distribution grid.

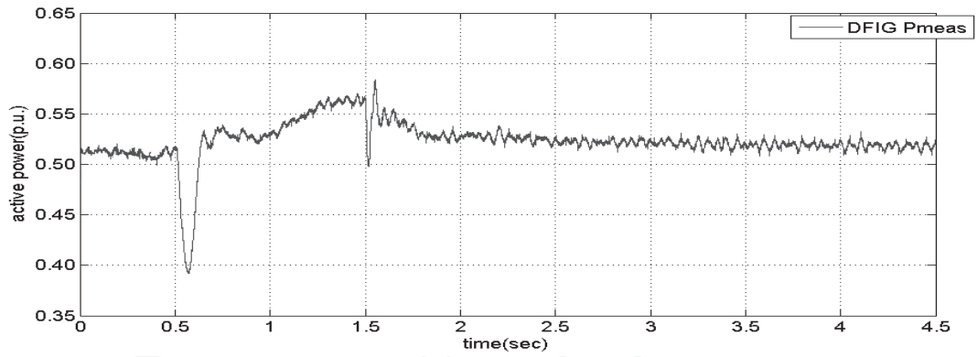

Fig. 33. The delivered active power by the WT with the DFIG.

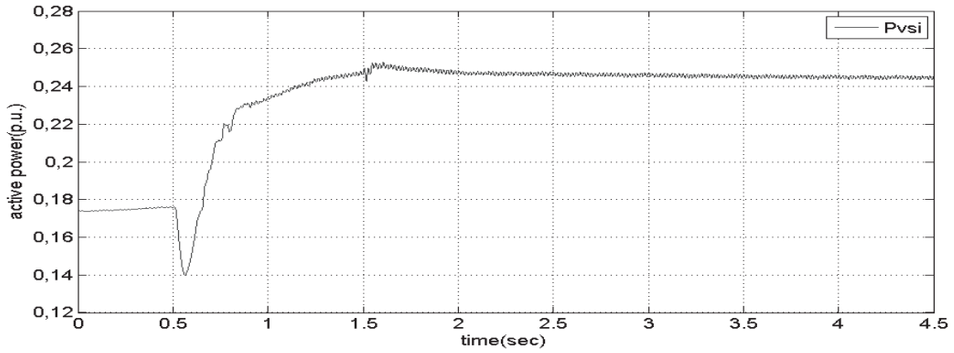

Fig. 34. The delivered active power by the hybrid FCS.

In Figs.35-37 the delivered reactive power by the grid, by the WT with the DFIG and by the hybrid FCS at the inverter's output are presented.

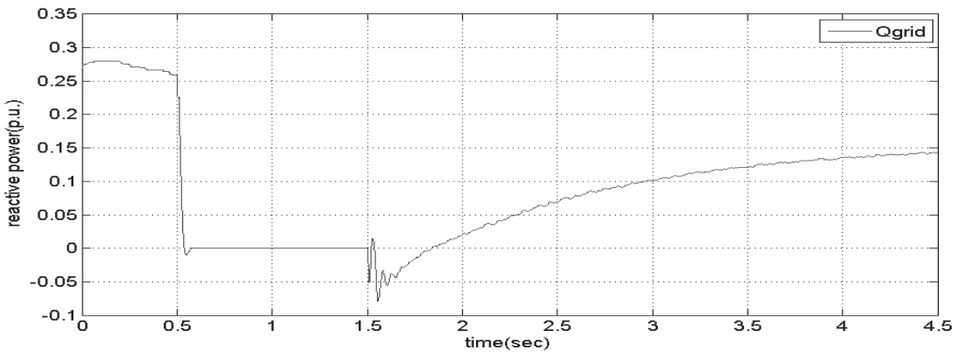

Fig. 35. The delivered reactive power by the weak distribution grid.

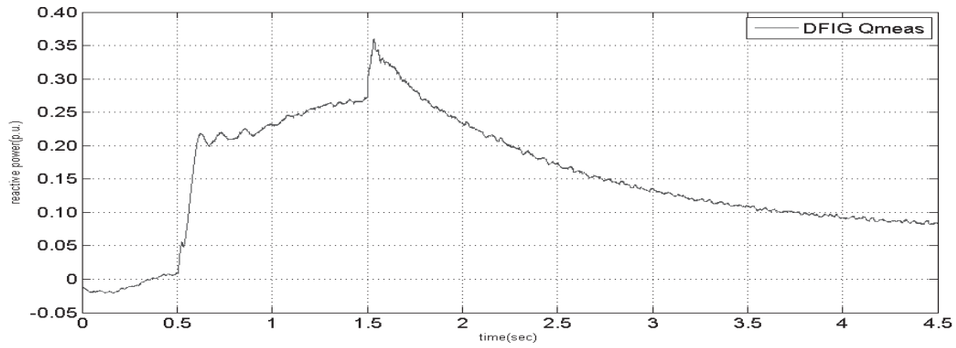

Fig. 36. The delivered reactive power by the WT with the DFIG.

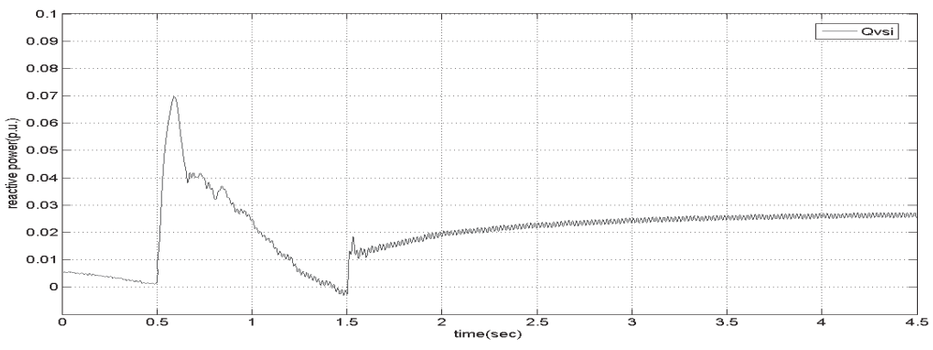

Fig. 37. The delivered reactive power by the hybrid FCS.

In Fig.38 the battery bank current is presented. The battery bank current increases rapidly, in order to supply the battery with the demanded power at 0.5 sec. At 1.5 sec, the battery bank continues to discharge and the current eventually returns to zero within 2.5 sec. In Fig.39, the FCS active power is presented. The FCS active power increases slowly in order to cover the total load demand and reaches a new steady state within 3 sec.

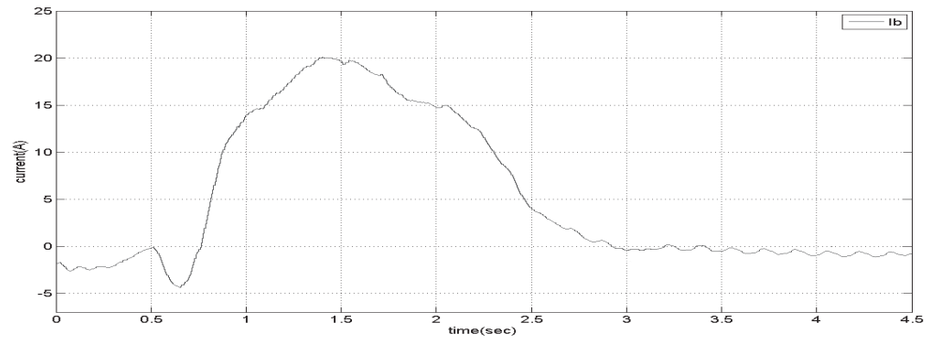

Fig. 38. The battery bank current in steady state and transient period.

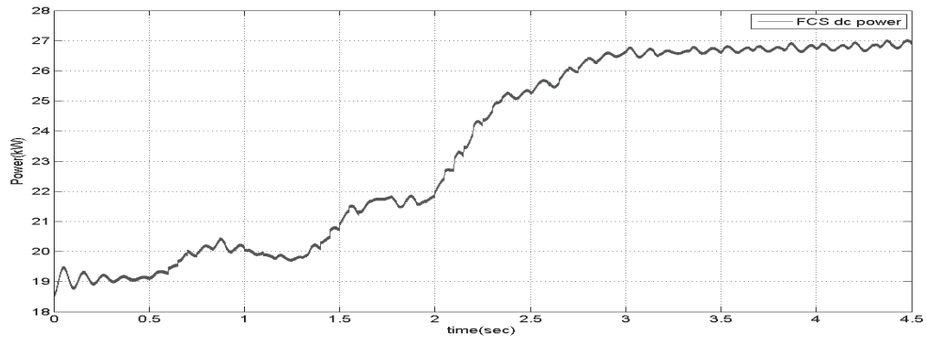

Fig. 39. The FCS active power delivered.

In Fig.40, the WT rotor speed is presented. Because of the disturbance imposed at the 0.5 sec and at 1.5 sec, the rotor looses kinetic energy and reaches a new steady state.

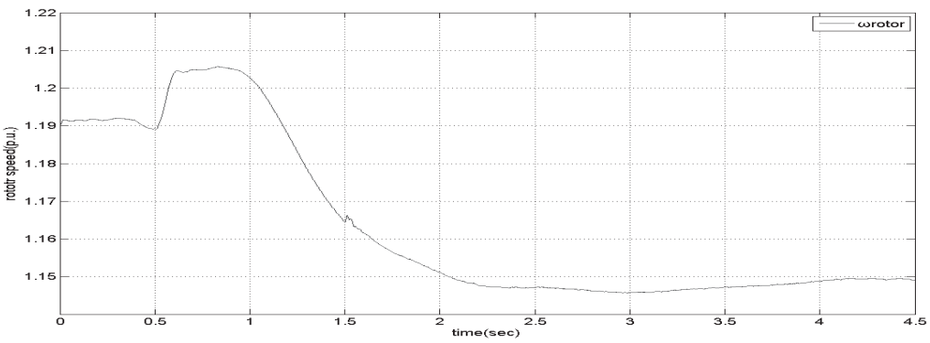

Fig. 40. The WT rotor speed in steady state and during transients.

In Fig.41, the control signals of the rotor side controller are presented in the same graph.

6. Conclusion

This chapter proposes a local controller based in fuzzy logic for the integration of a WT with DFIG into a micro-grid according to the «plug and play» operation mode. The designed

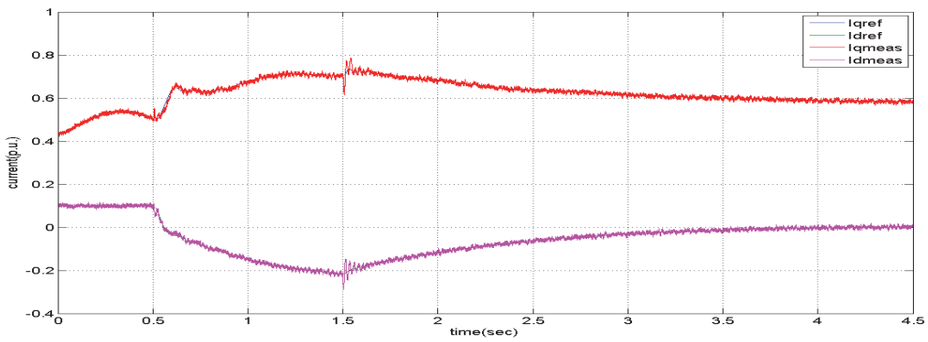

Fig. 41. the control signals of the rotor side controller.

controller is evaluated during local disturbances and during the transition from interconnected mode to islanding mode of operation either because of a fault at the mean voltage side or because of an intentional disconnection e.g. maintenance work. The simulation results prove that WT can provide voltage and frequency support at the distribution grid. The system response was analysed and revealed good performance. The proposed local controller can be coordinated with a micro-grid central controller in order to optimize the system performance at steady state.

7. Acknowledgment

The authors thank the European Social Fund (ESF), Operational Program for EPEDVM and particularly the Program Herakleitos II, for financially supporting this work.

8. References

Bathaee, S.M.T.; Abdollahi, M.H.(2007). Fuzzy-Neural Controller Design for Stability Enhancement of Microgrids, *Proceedings of UPEC 2007 42nd International Conference on Power Engineering*, pp. 562-569, ISBN 978-1-905593-36-1, Brighton, Sept. 4-6, 2007

Bousseau, P; Belhomme, R.; Monnot, E; Laverdure, N; Boëda, D; Roye, D; Bacha, S.(2006). Contribution of Wind Farms to Ancillary Services. CIGRE 2006 Plenary Session, Paris, report C6-103

Brabandere, K.De; Vanthournout, K.; Driesen, J.; Deconinck, G & Belmans, R. (2007). Control of Microgrids, *Proceedings of Power Engineering Society General Meeting IEEE,* pp. 1-7, ISBN 1-4244-1296-X, Tampa, June 24-28, 2007

Janssens, N. A.; Lambin, G; Bragard, N. (2007). Active Power Control Strategies of DFIG Wind Turbines, *Proceedings of IEEE Power Tech 2007*, pp. 516-521, ISBN 978-1-4244-2189-3, Lausanne Switzerland, July 1-5, 2007

Katirarei, F. & Iravani, M. R. (2006). Power Management Strategies for a Microgrid With Multiple Distributed Generation Units. *IEEE Transactions on Power Systems*, vol.21, No.4, (November 2006), pp.1821 – 1831, ISSN 0885-8950

Meiqin, M.; Chang, L.; Ming, D. (2008). Integration and Intelligent Control of Micro-Grids with Multi-Energy Generations: A Review, *Proceedings of ICSET 2008 on Sustainable Energy Technologies*,pp.777-780, ISBN 978-1-4244-1887-9, Singapore, Nov.24-27, 2008

Mohamed, Y. A. Ibrahim; El- Saadany, E. F.(2008). Adaptive Decentralized Droop Controller to Preserve Power Sharing Stability of Paralleled Inverters in Distributed Generation Microgrids, *IEEE Transactions on Power Electronics*, vol.23, No. 6, (November 2008) ,pp. 2806 – 2816, ISSN 0885-8993

Morren, J; de Haan, S; Kling, W; Ferreira, J.(2006) Wind turbines emulating inertia and supporting primary frequency control. *IEEE Transactions on Power Systems*, vol. 21, No. 1, (February 2006), pp 433-434, ISSN 0885-8950

Nikkhajoei, H.; Lasseter, R.H. (2009). Distributed Generation Interface to the CERTS Microgrid. *IEEE Transactions on Power Delivery*, vol. 24, No. 3, (July 2009), pp.1598 – 1608, ISSN 0885-8977

Nishikawa, K.; Baba, J.; Shimoda, E.; Kikuchi, T.; Itoh, Y.; Nitta, T.; Numata, S.; Masada, E. (2008).Design Methods and Integrated Control for Microgrid, *Proceedings of Power and Energy Society General Meeting - Conversion and Delivery of Electrical Energy in the 21st Century 2008 IEEE*, pp.1-7, ISBN 978-1-4244-1905-0, Pittsburgh, July 20-24, 2008

Shahabi, M.; Haghifam, M.R.; Mohamadian, M.; Nabavi-Niaki, S.A. (2009). Microgrid Dynamic Performance Improvement Using a Doubly Fed Induction Wind Generator. *IEEE Transactions on Energy Conversion*, vol.24, No.1, (March 2009), pp. 137-145, ISSN 0885-8969

Soultanis, N.L. (2008). *Contribution to the control and simulation of low voltage power systems with distributed generation*. PhD thesis, NTUA, Athens.

Fundamental and Advanced Topics in Wind Power
Edited by Dr. Rupp Carriveau

ISBN 978-953-307-508-2
Hard cover, 422 pages
Publisher InTech
Published online 20, June, 2011
Published in print edition June, 2011

As the fastest growing source of energy in the world, wind has a very important role to play in the global energy mix. This text covers a spectrum of leading edge topics critical to the rapidly evolving wind power industry. The reader is introduced to the fundamentals of wind energy aerodynamics; then essential structural, mechanical, and electrical subjects are discussed. The book is composed of three sections that include the Aerodynamics and Environmental Loading of Wind Turbines, Structural and Electromechanical Elements of Wind Power Conversion, and Wind Turbine Control and System Integration. In addition to the fundamental rudiments illustrated, the reader will be exposed to specialized applied and advanced topics including magnetic suspension bearing systems, structural health monitoring, and the optimized integration of wind power into micro and smart grids.

How to reference
In order to correctly reference this scholarly work, feel free to copy and paste the following:

Christina N. Papadimitriou and Nicholas A. Vovos (2011). Fuzzy Control of WT with DFIG for Integration into Micro-grids, Fundamental and Advanced Topics in Wind Power, Dr. Rupp Carriveau (Ed.), ISBN: 978-953-307-508-2, InTech, Available from: http://www.intechopen.com/books/fundamental-and-advanced-topics-in-wind-power/fuzzy-control-of-wt-with-dfig-for-integration-into-micro-grids

INTECH
open science | open minds

InTech Europe
University Campus STeP Ri
Slavka Krautzeka 83/A
51000 Rijeka, Croatia
Phone: +385 (51) 770 447
Fax: +385 (51) 686 166
www.intechopen.com

InTech China
Unit 405, Office Block, Hotel Equatorial Shanghai
No.65, Yan An Road (West), Shanghai, 200040, China
中国上海市延安西路65号上海国际贵都大饭店办公楼405单元
Phone: +86-21-62489820
Fax: +86-21-62489821

IntechOpen